Translation speed slowdown and poleward migration of western North Pacific tropical cyclones

npj | climate and atmospheric science

Article

Published in partnership with CECCR at King Abdulaziz University

https://doi.org/10.1038/s41612-024-00748-5

Translation speed slowdown and poleward migration of western North Pacific tropical cyclones

Xiangbo Feng [1,2]

Detecting and interpreting long-term changes in typhoon translation speed in observations remains challenging, contrasting with increased confidence in the poleward migration of typhoons. Here, I show a significant relationship between the basin-wide translation speed and the latitudinal position of tropical cyclones in the western North Pacific over 1980–2023. First, because tropical cyclones move faster at higher latitudes, the significant poleward migration (80 km/decade) increases the yearly basin-wide translation speed by 5% over the period. This effect reduces the detectability of a slowing trend. Second, the basin-wide translation speed solely contributed by regional translation speed has slowed by 18%, mostly in the late stage of the cyclone lifecycle. The translation speed slowdown and the poleward migration are likely caused by the same climate drivers through the interconnected large-scale atmospheric circulation between the tropics and subtropics. My findings suggest exacerbated tropical cyclone-related risk in the subtropical regions in a changing climate.

Tropical cyclone (TC) translation speed, which measures how fast TCs propagate across the Earth's surface, has a crucial impact on associated rainfall amounts and durations of hazard exposure. Recently, a global slowdown of TC translation speed in the Best Track observations since the 1950s was reported and hypothesised to be related to changes in large-scale atmospheric circulation caused by anthropogenic warming[1]. The western North Pacific (WNP; 0–60°N, 100–180°E), where TCs are also known in general as typhoons, has the largest slowing trend over this period (about −0.50 km/h per decade)[1]. Compared to intensity measurements, the track-based metrics, such as TC translation speed and track position, are less sensitive to the uncertainty in intensity identification techniques, which varies greatly with time and meteorological agencies[2–5]. However, data heterogeneity prior to the satellite era in the Best Track remains a major concern in detecting trends in TC translation speed and in attributing these changes to anthropogenic forcing. For example, the slowdown since the 1950s has been questioned due to potential undercounting of tracks in the subtropics in the early years[6,7]. Other studies[6–10] found that TC translation speed in the WNP does not exhibit a significant change throughout the satellite era (since 1980) when using the Best Track data that are considered to be more reliable. Interdecadal climate variability was also found to affect the trend detection in TC translation speed[8,11]. Thus, identifying a robust trend signal in translation speed of WNP TCs in observations is challenging. Since the aforementioned studies, the Best Track data in the satellite era have now extended by 4–7 years, which help to identify a robust long-term trend in translation speed emerging from climate variability.

Furthermore, because the trend detection is usually estimated by averaging translation speed values of individual storms over the entire ocean basin (i.e. the basin-wide translation speed), it is unknown whether any identified trends, if they exist, are due to a basin-wide systematic change or due to region-scale changes[12]. Knowing spatial variations of the translation speed changes will help to understand the robustness and the sensitivity of the TC changes to long-term climate drivers. The large-scale atmospheric circulation in the tropics and extra-tropics, in which TCs form and travel, has changed in recent decades, very likely forced by anthropogenic climate change[13–24]. Thus, establishing an evident and quantitative long-term relationship between TC translation speed and the large-scale circulation, which is consistent with the cascade understanding of atmospheric processes in a warming climate, will increase our confidence in future projections of TCs and their impacts.

Contrasting with no consensus in the long-term trends of TC translation speed in the WNP, there is a better agreement in the trends of TC latitudinal position[12]. The annual average location of WNP TCs (i.e. the basin-wide position) was found to migrate poleward over the satellite era[25–27]. A poleward trend was also simulated in general circulation models with anthropogenic forcing[26,28]. Recent study[29] further showed that not only

[1]National Centre for Atmospheric Science and Department of Meteorology, University of Reading, Reading, UK. [2]Department of Physics, Imperial College London, London, UK. e-mail: xiangbo.feng@reading.ac.uk

have the locations of TC genesis and lifetime-maximum intensity significantly shifted north, as shown in earlier studies, but so too have all track-points, confirming a systematic northward migration of WNP TCs over the satellite era. Because TCs usually propagate faster when moving to higher latitudes of the basin, a systematic northward migration of track could cause the basin-wide translation speed to increase. This increasing trend related to the concurrent changes in storm position could reduce the detectability of a slowing trend in the basin-wide translation speed if it exists. Fundamental science question is: are the translation speed slowdown and the poleward shift of WNP TCs linked, suggesting the common climate drivers? This paper will utilize the increased confidence in the poleward migration of WNP TCs to evaluate the robustness of the translation speed change since 1980.

Here, I examine the coexistent trends in the basin-wide translation speed and the latitudinal position of WNP TCs using updated observations during 1980–2023. The interannual co-variability between the two metrics of TC track is also examined to build confidence for the plausible linkages between the two coexistent trends. Essentially, I partition the basin-wide translation speed into two main components, which are solely due to the poleward migration of TC track and due to regional changes in translation speed, respectively. This analysis separates a "ground" change of TC translation speed from the interference of the track shift. The coexistent trends in translation speed and position are then linked to the ambient large-scale atmospheric circulation. This study uses the latitudinally homogenised Best Track data from the Japan Meteorological Agency (JMA), and it minimizes the effect of long-range climate variability on TC metrics and environment by fitting a multivariate regression as suggested in refs. 25,26,29. In principle, the Best Track data justification is based on the sampling coverage of track in the subtropics[6,7] where translation speed in the late stage of the TC lifecycle (i.e. after the extratropical transition) exhibits the most robust long-term changes. The changes of the basin-wide translation speed are small in other sources of Best Track data in which the track e.g. after the extratropical transition is undercounted. See the Methods section for details on the data and methodologies.

Results

Translation speed slowdown and poleward migration of TCs

First, I show the trends in the basin-wide translation speed and latitudinal position of WNP TCs in the Best Track over the past 44 years (1980–2023). The translation speed and storm position are estimated from the 6-hourly track points during the whole lifetime of storm. The annual-mean basin-wide translation speed has a statistically significant slowdown over the period (Fig. 1). The slowing rate is −0.63 ± 0.37 km/h per decade (±representing the 95% confidence interval of trend value, see "Statistical analyses" in the Methods section). This corresponds to 13% reduction of translation speed with respect to the 44-year mean. This trend value is higher than the observed rate (−0.50 km/h per decade) over 1949–2016[1], in which the confidence in the data homogeneity is low[6,7], but the difference is not statistically different (within the uncertainty range). In the meantime, with the same data, the basin-wide latitudinal position of TCs during the whole lifetime is significantly shifting poleward by 80 ± 32 km per decade, i.e. by ~350 km over the whole period (Fig. 1). This migrating rate is close to the observed rate (78 km per decade) over a similar period (1979–2018)[29]. After removing linear trend (i.e. detrending), the interannual variability of the basin-wide translation speed and latitudinal position is negatively correlated (Supplementary Fig. 1a), with $r = -0.22$, but the correlation is not significant at 95% confidence (see "Statistical analyses" in the Methods section). This insignificant co-variability in the translation speed and latitudinal position is caused by the opposite relationships between the poleward shift and the two main components of the basin-wide translation speed (this will be discussed in the next section).

Next, I evaluate the long-term trends in translation speed and track density in the latitude bands. There is distinct spatial inhomogeneity in the climatology of translation speed. In the WNP, TC translation speed is latitude-dependent, with faster speed in the subtropics and slower speed in the tropics (Fig. 2a). TC track density represents the number of 6-hourly track points in a latitude band, per year, while the proportion of track density is the percentage of the track density in a latitude band over the total number of track points in the whole basin. In the WNP, TCs usually travel westward or west-northward along the large-scale easterly steering flows on the equatorward side of the Western North Pacific Subtropical High (WNPSH) (Supplementary Fig. 2). Many of the storms start recurving north with a reduced translation speed on the western edge of the WNPSH, and then in the late stage of the lifecycle (e.g. in the extratropical cyclone phase) they turn east in conjunction with the fast-moving westerly jet in the subtropics. The proportion of track density is climatologically highest at 20°N where storms are about to recurve (i.e. at slow translation speeds).

Figure 2b shows the observed trends in translation speed and track density in various latitude bands over the 44 years. Significant slowdown up to −2.0 km/h per decade is found in the latitude band of 20–40°N. Slowdown is also found in other regions, but the trends are not statistically significant. Over the period, TC track density has a significant decreasing trend (−40 ~ −10 number/decade accumulated in a 10° latitude band) in the tropics (0–20°N), due to a reduction of the frequency of low-latitude TCs (Supplementary Fig. 3), consistent with previous study[29]. Figure 2b further shows the changes in the proportion of TC track density in the latitude bands. Compared to the track density, the proportion of track density has a clearer north-south contrast in trend (i.e. a seesaw-like change). It has a significant increasing trend in the north of 20°N (up to 2.2%/decade accumulated in a 10° latitude band) and a significant decreasing trend in the south of 20°N (up to −3.8%/decade accumulated in a 10° latitude band). In the subtropics, although the track density itself has no significant trends, when it is divided by the annual track points that has a decreasing trend associated with fewer storms (Supplementary Fig. 3), the trend of the proportion becomes increasing and significant (Fig. 2b). I further find that the translation speed trend in the subtropics is caused by the recurving TCs that usually travel further north, whilst the seesaw-like trends in regional track density along the latitude are seen in both recurving and non-recurving TCs (Supplementary Fig. 4a–d). Over 80% of recurving TCs in the basin underwent the extratropical transition and became extratropical cyclones[30]. When track points in this late stage of the lifetime are excluded, the translation speed trend in the subtropics largely reduces (Supplementary Fig. 4e, f). Geographically, these changes in TC translation speed and track density are confined to the west sector of the basin (100–140°E) (Supplementary Fig. 5a, b). Northeast Asia (i.e. north China, Korea, and Japan) and its marginal seas affected by recurving TCs saw the largest slowing trend in TC translation speed. TC translation speed has no significant trends in the east sector of the basin (140–180°E) where the track sampling number is climatologically low.

The seesaw-like trends in relative track density (Fig. 2b) determine the trend in the basin-wide latitudinal position (Fig. 1). In the past 44 years, the north tracks give an increasing weighting to the basin-wide TC statistics, whilst the south tracks give a decreasing weighting to the basin-wide statistics. On the yearly basis, the basin-wide latitude of TCs can be expressed as an accumulation of the latitude bands weighted by the relative track density (see "Decomposing the basin-wide translation speed" in the Methods section). Thus, the northward shift of the latitudinal position can be understood as an increase of the proportion of north tracks. With the same concept, for the basin-wide translation speed, the northward migration of tracks will give a greater weight to TCs in the subtropics where storms climatologically propagate faster and will give a less weight to TCs in the tropics where storms climatologically propagate slower (Fig. 2b).

Slowing trend in the basin-wide translation speed

In this subsection, by considering the counteracting effect of the track displacement, I recalculate the basin-wide translation speed of TCs in the whole lifecycle. The basin-wide translation speed is understood as the aggregation of regional translation speed weighted by the relative track density throughout the whole latitude range (see "Decomposing the basin-wide translation speed" in the Methods section). Therefore, I partition the basin-

wide translation speed into three components on the yearly basis, to quantify the contributions of the northward migration of track density (denoted as $\delta_{p'}$), the changes in regional translation speed ($\delta_{TCS'}$), and the co-variations of regional track density and regional translation speed ($\delta_{p'TCS'}$). For each year, in principle, the component $\delta_{p'}$, determined by track position, retains the trend and interannual variability in the relative track density at each latitude band and holds unchanged climatology of regional translation speed. The component $\delta_{TCS'}$, determined by regional translation speed, retains the trend and interannual variability in regional translation speed and holds unchanged climatology of the relative track density. The component $\delta_{p'TCS'}$ informs the interannual co-variability of regional track density and regional translation speed. Using this partitioning method, the budgets of the interannual variability and trend in the basin-wide translation speed is balanced (Supplementary Tables 1 and 2). As $\delta_{p'TCS'}$ is a small term and has no trend found, it is not shown in the Results.

Figure 3 shows the annual values of the first two components of the basin-wide translation speed. The basin-wide translation speed due to track changes ($\delta_{p'}$) has a significant upward trend of 0.23 ± 0.17 km/h per decade, i.e. 5% increase with respect to the 44-year mean. In contrast, the basin-wide translation speed due to changes in regional translation speed ($\delta_{TCS'}$) has a significant downward trend of –0.88 ± 0.45 km/h per decade, i.e. 18% reduction with respect to the 44-year mean. The upward trend in $\delta_{p'}$ counteracts the downward trend in $\delta_{TCS'}$, reducing the overall trend to –0.63 ± 37 km/h per decade (Fig. 1). The detrended interannual variability of the basin-wide TC latitude is strongly correlated with the detrended $\delta_{p'}$ ($r = 0.73$) and anti-correlated with the detrended $\delta_{TCS'}$ ($r = -0.45$)

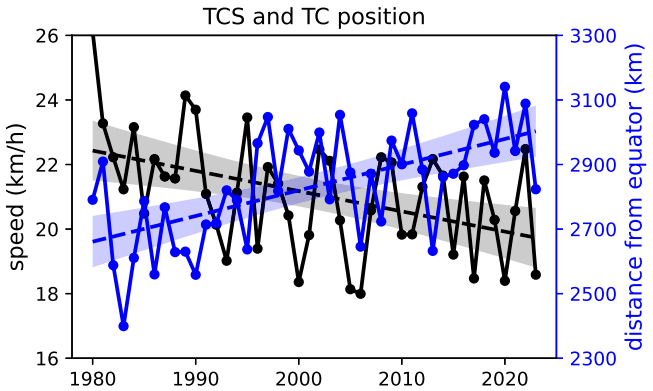

Fig. 1 | Basin-wide translation speed and latitudinal position of tropical cyclones in observations. Annual-mean values of tropical cyclone translation speed (TCS, black) and tropical cyclone latitude (TC position, blue) in the western North Pacific over 1980–2023, from the 6-hourly track points in the Best Track. Dashed lines represent the linear trend, with shading showing 95% confidence interval for the linear fit.

(Supplementary Fig. 1b, c). These confirm that the overall trend of the basin-wide translation speed in Fig. 1 is related to the regional changes in both translation speed and track position.

I further decompose the translation speed into latitudinal and longitudinal components by only considering the latitudinal or longitudinal movements (Fig. 4; trend values provided in Supplementary Table 1). At the basin-wide scale, the overall longitudinal translation speed has a significant slowing trend (–0.67 ± 0.30 km/h per decade), which predominates the slowing trend in the total translation speed (–0.63 ± 37 km/h per decade), while the overall latitudinal translation speed has no trend. I further confirm that the significant slowdown of the longitudinal translation speed is caused by the $\delta_{TCS'}$ term (–0.74 ± 0.38 km/h per decade). The $\delta_{TCS'}$ term of the longitudinal translation speed explains 84% of the slowing trend in $\delta_{TCS'}$ of the total translation speed (–0.88 ± 0.45 km/h per decade). The slowdown of the basin-wide $\delta_{TCS'}$ in Fig. 4 is caused by the slowing trends restricted to the subtropics (20–40°N) (Supplementary Fig. 6), consistent with the changes in the total translation speed (Fig. 2b). It is worth noticing that the trend of the latitudinal translation speed due to the poleward migration ($\delta_{p'}$; 0.27 ± 0.11 km/h per decade) is larger than that of the longitudinal translation speed (0.05 ± 0.13 km/h per decade). This is because the climatology of the latitudinal translation speed has a unimodal distribution along the latitude while the climatology of the longitudinal translation speed has a bimodal distribution (Supplementary Fig. 6). This allows the poleward migration of track to have a larger impact on the basin-wide latitudinal translation speed than on the basin-wide longitudinal translation speed.

In short, over 1980–2023, after excluding the counteracting effect of the poleward shift of track, the slowing rate of the basin-wide translation speed of TCs changes from –0.63 ± 0.37 km/h per decade to –0.88 ± 0.45 km/h per decade. Thus, the poleward shift of track has a clear impact on the trend detection in the basin-wide translation speed. The detrended interannual co-variability suggests that the remaining translation speed ($\delta_{TCS'}$) is strongly associated with the average location of TCs ($r = -0.45$, Supplementary Fig. 1c), indicating that the coexistent trends in these two metrics are likely caused by the same climate drivers.

Changes in subtropical and tropical large-scale circulation

In this subsection, I employ large-scale circulation to interpret the relationship between the translation speed and the latitudinal position of TCs in observations (Fig. 3b). In the WNP, TC movement is mostly steered by the large-scale background steering flow along the edges of the WNPSH (Supplementary Fig. 2). Here, the large-scale background steering flow is defined as the average winds in the middle troposphere, and the annual large-scale steering flow is the average of monthly steering flow in the whole year but weighted by the monthly climatology of WNP TC frequency (referred to as seasonality-weighted average, see "Large-scale environmental conditions" in the Methods section). Over the past 44 years, the large-scale background steering flow has changed (Fig. 5a). The subtropics (20–40°N) of the WNP, where TC translation speed is slowing (Fig. 2b), saw a slowing

Fig. 2 | Climatology and long-term changes in translation speed and track density of tropical cyclones at the latitude bands in observations. **a** Climatology of tropical cyclone translation speed (TCS, blue), track density (magenta), and the proportion of track density (red), at the 10° latitude-moving bands from 0 to 60°N, in the western North Pacific over 1980–2023, from the 6-hourly track points in the Best Track. **b** Linear trends of TCS (blue), track density (magenta), and the proportion of track density (red), at the 10° latitude-moving bands from 0 to 60°N, in the western North Pacific over 1980–2023, from the 6-hourly track points in the Best Track. In (**b**) thick solid lines show significant trends at 95% confidence, thin dashed lines for insignificant trends at 95% confidence.

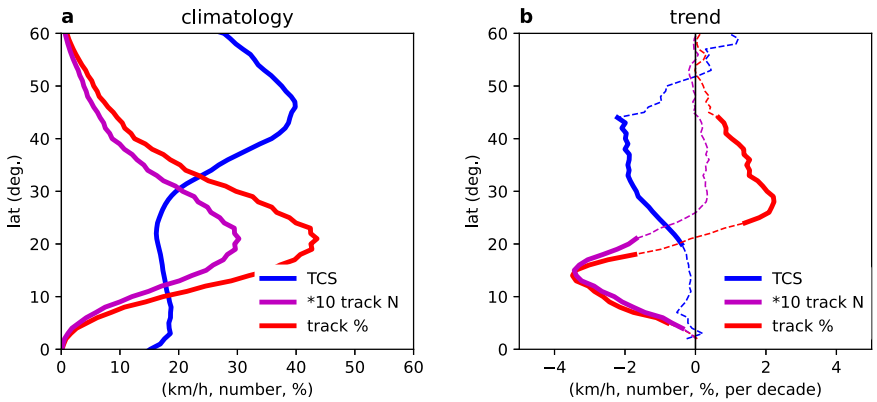

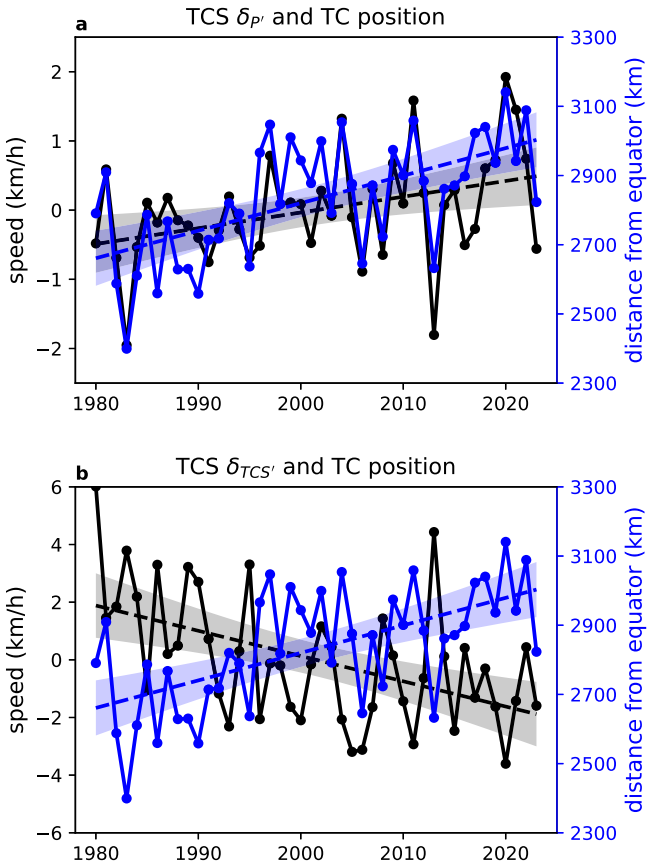

Fig. 3 | Basin-wide translation speed of tropical cyclones due to track shift and due to regional translation speed changes in observations. a Annual deviations of basin-wide tropical cyclone translation speed (TCS) related to track shift ($\delta_{P'}$, black), and annual values of tropical cyclone latitude (TC position, blue), in the western North Pacific over 1980–2023, from the 6-hourly track points in the Best Track. **b** as (**a**), but with black line for annual deviations of basin-wide TCS related to regional TCS change ($\delta_{TCS'}$). Dashed lines represent the linear trend, with shading showing 95% confidence interval for the linear fit.

of the prevailing westerly winds. The average changing rate of the large-scale background steering flow in the west sector of the subtropics (20–40°N, 120–160°E), where TC track density is high in this latitude band (Supplementary Fig. 2c) and TC translation speed is slowing (Supplementary Fig. 5b), is –0.85 ± 0.43 km/h per decade (Supplementary Fig. 7a). This is close to the slowing rate of $\delta_{TCS'}$ of the longitudinal translation speed (–0.74 ± 0.38 km/h per decade). Thus, the slowing of the basin-wide longitudinal translation speed, which dominates the slowing of the total translation speed of TCs as mentioned above, can be explained by the slowing of the large-scale steering flow in the subtropics. The detrended interannual correlation between the large-scale background steering flow in this sector and the longitudinal $\delta_{TCS'}$ is significant at 95% confidence ($r = 0.31$). This correlation value indicates that other factors (e.g. the Beta drift) may also affect the degree to which the interannual variability of TC translation speed can be explained by the large-scale background steering flow (this will be discussed in the Discussion section).

Within the latitude bands, the significant slowing rates of the longitudinal translation speed of TCs (Supplementary Fig. 6b) are close to the slowing rate of the westerly steering flow in the west sector (about 1–2 km/h per decade; Fig. 5a). Because of no trend in the southerly steering flow, the slowing of the latitudinal translation speed (about 1 km/h per decade; Supplementary Fig. 6b) could be related to a northerly change in the upper-tropospheric winds (Fig. 5c). This generally agrees with the expectation that after the recurvature point, TCs, which undergo the extratropical transition, are strongly affected by the upper-tropospheric winds[30–32]. Similarly, the middle- and upper-tropospheric winds can also explain the slowing rates of the two components of translation speed at the regional scales (Supplementary Fig. 5c, d).

The slowing of the steering flow in the subtropics is associated with an increase of middle-tropospheric geopotential height in the middle latitudes (40–60°N) and a decrease in the low latitudes (0–20°N), relative to the global mean (Fig. 5a). This disproportional north-south change in geopotential height is also accompanied with an amplified warming of sea surface temperature (Fig. 5b) and of middle-tropospheric air temperature in the subtropics (Supplementary Fig. 8a). In contrast, there is an opposite north-south change of temperature in the upper troposphere (Supplementary Fig. 8b). The detrended interannual variability of the large-scale steering flow is positively correlated with both the temperature gradient and the geopotential height gradient between the middle and low latitude bands (Supplementary Fig. 9), with $r = 0.36$ and 0.31 (both significant at 95% confidence), respectively. Thus, the slowing of the large-scale steering flow is associated to the disproportional warming in the low-to-middle troposphere between the tropical and subtropical regions. This finding is consistent with the weakening of large-scale circulation in the middle latitudes by assuming a warming climate[14–16]. To ensure that the above changes in environmental conditions are independent of TC changes, I calculated the reverse seasonality-weighted annual average of environment (see "Large-scale environmental conditions" in the Methods section). This annual average gives most weight to monthly environment values when TCs are climatologically rare and least weight to environment values when TCs are climatologically active. I found that, after minimizing the impact of TC presence using this method, the aforementioned long-term changes in large-scale steering flow and associated environmental conditions remain robust and these changes even tend to be larger (Supplementary Figs. 7b, 10).

Now, I propose plausible linkages between the slowing of the large-scale steering flow and the poleward migration of TCs. They could be bridged through three pathways. First, related to the slowing of the steering flow in the subtropics and the associated weakening of the southern branch of the WNPSH (Fig. 5a, Supplementary Fig. 2a), which is also seen as a poleward shift of the WNPSH system, TCs formed in the low latitudes are more likely to travel towards northwest or recurve north rather than travel straight west. In other words, due to its changes, the WNPSH opens a wider "entrance gate" for the cyclones of tropical origin to enter the subtropics.

Second, in the subtropics, vertical wind shear has significantly reduced over the past four decades, driven by the easterly trends of the upper-level winds (Fig. 5c). This change in the upper-level winds is well depicted by the slowing of the mid-level large-scale steering flow (Fig. 5a). Together with increases in sea surface temperature (SST; Fig. 5b) and mid-level relative humidity (Supplementary Fig. 8c), the environmental conditions in the subtropics become more favourable for TCs to maintain. This means that once TCs have entered this region, they are more likely to live longer, thus giving more weight to north tracks.

The third factor is the strengthening of the Pacific Walker Circulation (PWC) in the past 44 years. The strengthening of the PWC is seen in both the low-level zonal winds in the central equatorial Pacific (Fig. 5b) and the sea-level pressure gradient over the eastern equatorial Pacific and the Indo-Pacific warm pool (Fig. 5d). The latter is widely used as an index to measure the strength of the PWC (see "Climate and Walker Circulation indices" in the Methods section). A recent strengthening of the PWC has been reported in other observational studies as well[17–22,29]. Related to reduced relative vorticity in the lower troposphere and increased vertical wind shear in the central equatorial Pacific (Fig. 5b, c), a stronger PWC suppresses TC generation in the deep tropics, thus decreasing the proportion of low-latitude tracks and increasing the proportion of north tracks over the whole basin (Fig. 2b). The seesaw-like changes in relative track density due to the PWC strengthening is the main driver of the poleward migration of WNP TC tracks in the past four decades[29].

The interannual correlation between the detrended PWC index and the detrended large-scale background steering flow in the northwest sector

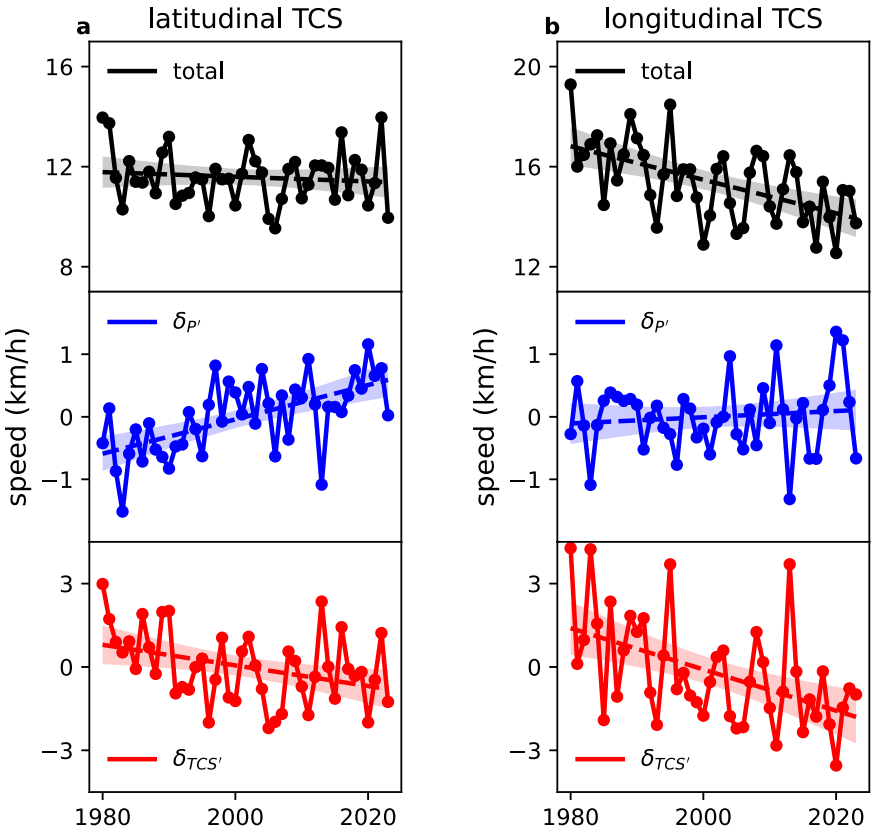

Fig. 4 | Basin-wide latitudinal and longitudinal translation speed of tropical cyclones due to track shift and due to regional translation speed changes in observations. a Annual values of tropical cyclone latitudinal translation speed (latitudinal TCS, black), annual deviations of latitudinal TCS related to track shift ($\delta_{P'}$, blue), and annual deviations of latitudinal TCS related to regional TCS change ($\delta_{TCS'}$, red), in the western North Pacific over 1980–2023, from the 6-hourly track points in the Best Track. **b** as (**a**), but for longitudinal translation speed (longitudinal TCS). Dashed lines represent the linear trend, with shading showing 95% confidence interval for the linear trend.

(20–40°N, 120–160°E) is not statistically significant ($r = -0.20$). However, I find that the large-scale steering flow in the wider subtropical region (20–60°N, 120–180°E) is significantly correlated with the PWC index (Fig. 5d), with detrended correlation $r = -0.34$. I further calculate the regression of large-scale environmental conditions onto the PWC index after removing the effects of the long-range trend and climate variability (Fig. 6). Clearly, in years when the PWC is anomalously strong, the large-scale steering flow has easterly anomalies in the northern branch of a weakened WNPSH centred at 20°N (Fig. 6a). This means that on the yearly basis, a strengthening of the PWC occurs with a significant slowdown of the subtropical steering flow in which recurving TCs are embedded. The interannual fluctuation of the PWC is associated with the east-west gradient of SSTs in the equatorial Pacific (Fig. 6b) and the low-level easterly wind anomalies in the central equatorial Pacific, i.e. a La Niña-type pattern. Importantly, these large-scale dynamical and thermodynamical anomalies associated with the fluctuated PWC index largely resemble the long-term trends over the past 44 years especially in the subtropics (Fig. 5a, b). This indicates that the coexistent long-term changes in the PWC and the subtropical steering flow (Fig. 5d) are likely caused by the same internal or external drivers and that these changes could be linked via the dynamical pathways as occurred at the interannual timescales. The coexistent changes in the PWC and the subtropical steering flow is also found in the reverse seasonality-weighted annual average of environment (with detrended correlation $r = -0.54$; Supplementary Fig. 10d), confirming the above conclusion. Further studies with sensitivity experiments based on climate models that are constrained with long-term drivers are needed to better understand and detangle the cascading process responsible for the associated trends in the tropical and subtropical circulations. It might be related to the regional Hadley circulation or large-scale vorticity advection in upper troposphere. Nevertheless, over the past 44 years, the translation speed slowdown and the poleward migration of WNP TCs, due to the changes in the steering flow and the PWC, are hypothesized to be linked by the large-scale circulation connecting the tropics and subtropics.

Discussion

There is still lack of consensus in long-term changes in translation speed of WNP TCs in observations. In contrast, the climate research community has increased confidence in the northward migration of WNP TC track and more confidence in the response of large-scale circulation, in which TCs are embedded, to anthropogenic warming. Here, using the JMA Best Track data that best sample the subtropical region of the WNP, I showed observed evidence that in the satellite era (1980–2023) the basin-wide translation speed of WNP TCs has significantly slowed. I found that the change of TC translation speed is closely related to the poleward migration of storms. The poleward migration of TCs (80 ± 32 km per decade) gives relatively greater weight to higher-latitude TCs that travel climatologically faster and give less weight to lower-latitude TCs that travel climatologically slower. This effect increases the yearly basin-wide translation speed by 5% over the period. After the effect of the poleward migration is detached, I found that in the past 44 years, the basin-wide translation speed has slowed by −0.88 ± 0.45 km/h per decade, i.e. 18% reduction over the period. This robust and fast slowing trend is explained by the slowing of the large-scale steering flow in the subtropics associated with the disproportional warming between the low and middle latitudes. This finding supports the hypothesis that the changes in large-scale atmospheric circulation in the subtropics are key to the response of TC translation speed to long-range climate drivers such as internal variability and anthropogenic warming.

The observed poleward shift of TC track can be plausibly related to the slowing of the large-scale steering flow in the subtropics as well. With a slowing of the large-scale steering flow in the subtropics, the environmental conditions in the subtropics become more favourable for TCs to recurve north and maintain longer, while the environmental conditions in the deep tropics become less favourable for TCs to form, causing the overall location of TCs to shift northward. I found that these environment changes in the tropics and subtropics favoring the poleward migration of TCs are further linked to the strengthening of the PWC, confirming recent studies[17–22,29]. But it remains unclear how fast the coexistence of the trends in the PWC and the

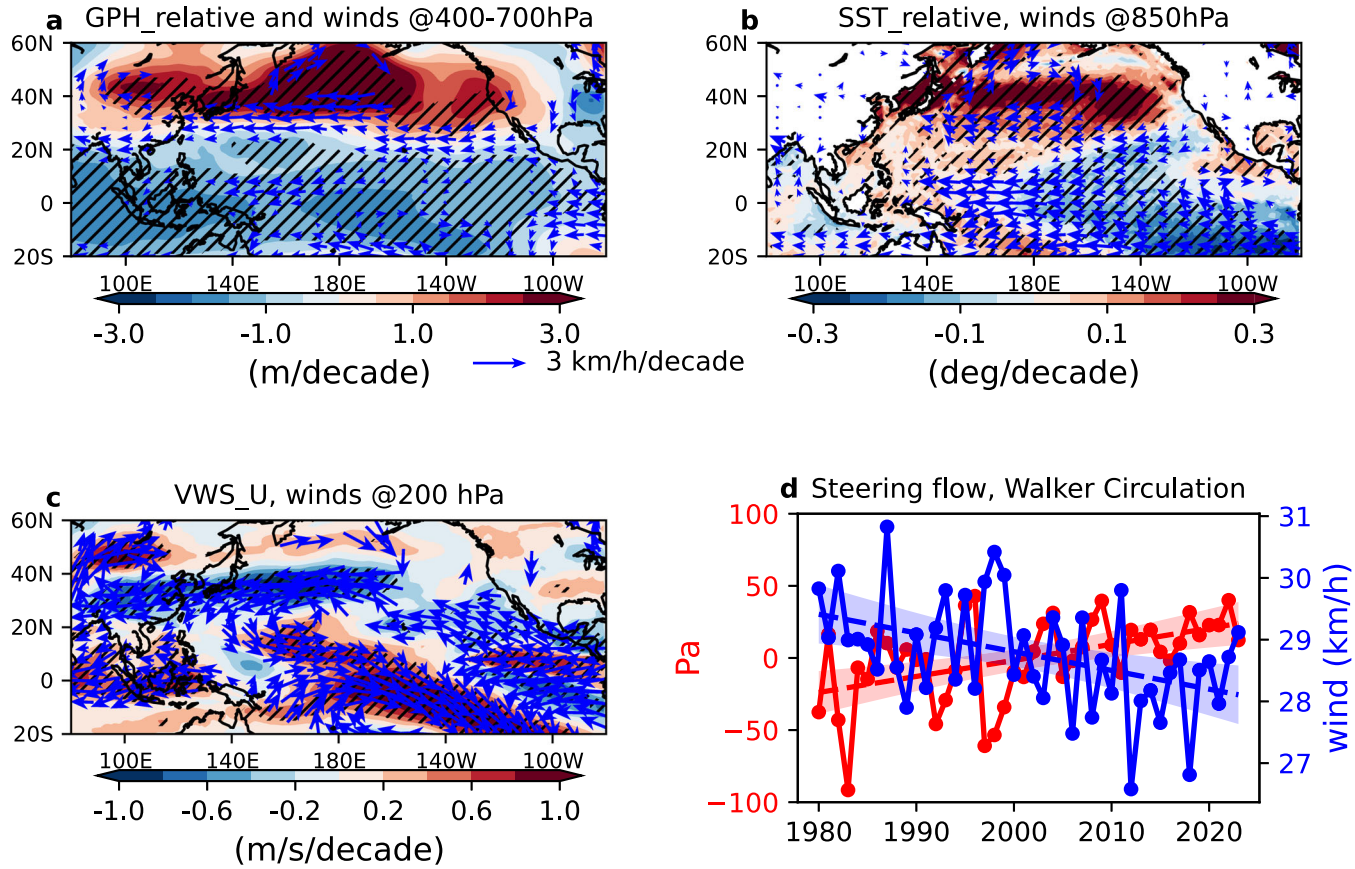

Fig. 5 | Long-term changes in large-scale atmospheric circulation and environment. a Linear trends of annual geopotential height relative to the global mean (GPH_relative, shading) and annual large-scale steering winds (vectors) averaged over 700, 600, 500, and 400 hPa, over 1980–2023, in ERA5. **b** as (**a**), but for sea surface temperature (SST, shading) and 850hPa winds (vectors). **c** as (**a**), but for zonal vertical wind shear (VWS_U, shading) and 200hPa winds (vectors). Hatched areas and vectors in (**a**–**c**) show significant trends at 90% confidence. **d** Annual values of the Pacific Walker Circulation index (red) and the subtropical large-scale steering winds in the WNP, over 1980–2023, in ERA5. In (**d**), dashed lines represent the linear trend, with shading showing 95% confidence interval for the linear trend. The Pacific Walker Circulation index is defined as the east-west difference between the annual sea-level pressure averaged over the central and eastern equatorial Pacific (160°W–80°W, 5°S–5°N) and over the equatorial Indian Ocean and western equatorial Pacific (80°E–160°E, 5°S–5°N), while the subtropical large-scale steering flow is the large-scale steering winds averaged in the subtropical region of the WNP (20–60°N, 120–180°E). The annual circulation and environment are calculated by averaging the monthly data weighted with the seasonality of WNP TC frequency throughout the 12 months.

subtropical steering flow is emerging in a changing climate. Further analysis and sensitivity experiments are required to better understand the linkages between the large-scale circulation in the subtropics and tropics and whether the relationship will be held in the future. This will increase our confidence in projecting TC-related hazard exposure for the future.

This study highlights the coexistence of the translation speed slowdown and the poleward migration of WNP TCs over the past 44 years. Northeast Asia (i.e. north China, Korea, and Japan) saw the largest slowing trend in TC translation speed when TCs are in the late stage of the lifecycle. Accumulation of TC rainfall in these regions is likely enhanced due to the slowing translation speed. This implies that TC-related climate risk is becoming higher in the subtropical regions.

I notice that the detection of long-term trends in TC translation speed is sensitive to the sampling of the Best Track data in the subtropics. Best Track data from other agencies have also been evaluated in this study (see "Best Track data and data justification" in the Methods section). In other sources of Best Track data, due to sparse sampling coverage in the extratropical cyclone phase (after the extratropical transition of TCs is complete)[33], the slowing trend of TC translation speed is not robust. This confirms the recently raised concern about the suitability of heterogeneous data in deriving a long-term trend in TC translation speed[6,7]. This also means that the long-term change in TC translation speed in this study is sensitive to the stages of the TC lifecycle. In the WNP, when a TC recurves to the middle latitudes, it usually (80% chance) undergoes the extratropical transition[30]. A cyclone undergoing or even completing the extratropical transition can continue to pose a serious threat to coastal and maritime activities. Thus, it is important to consider all stages of the TC system when TC-related climate risk is evaluated in a climate change context.

In this study, the slowing rate of TC translation speed is interpreted by the long-term change in the large-scale steering flow, with the assumption that the flow would exist in the absence of the storm. TC propagation is also influenced by TC itself via the Beta drift that would not exist in the absence of the storm[34]. The Beta drift, climatologically accounting for 10–20% of TC translation speed[35–37], is associated with storm size and intensity[38], and more complicatedly it is not independent of the large-scale environmental flow[34,36,37]. The Beta drift may be responsible for the discrepancies in the interannual variability between the translation speed and the large-scale steering flow (Supplementary Fig. 7a). However, because a significant change in the large-scale steering flow is also seen in seasons when TCs are climatologically inactive, the Beta drift is not expected to alter the conclusions. Another noteworthy issue is the nonlinear evolution of the climate teleconnections in a warming climate. In this study, the trend detection and interannual correlation are made after removing the effect of two dominate climate modes in the basin (namely the El Niño Southern Oscillation and the Pacific Decadal Oscillation) by assuming the teleconnections are stationary with time. Studies[39–41] show that these climate teleconnections are

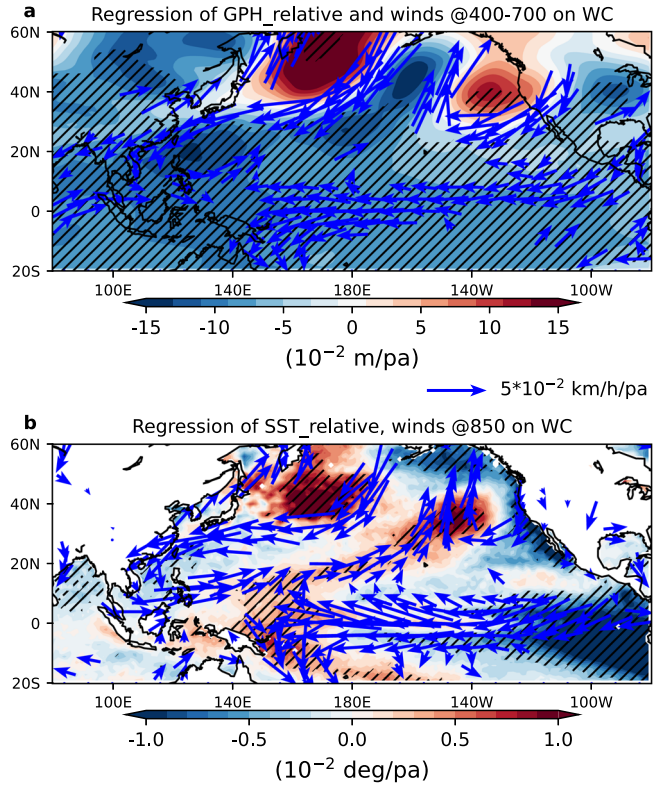

Fig. 6 | Regression of large-scale atmospheric circulation and environment onto the Pacific Walker Circulation index after removing trend. a Regression coefficients of annual geopotential height relative to the global mean (GPH_relative, shading) and annual large-scale steering winds (vectors) averaged over 700, 600, 500, and 400 hPa, onto the Pacific Walker Circulation (WC) index, over 1980–2023, in ERA5. Linear trend has been removed from all the variables before the regression fitting. **b** as (**a**), but for sea surface temperature (SST, shading) and 850 hPa winds (vectors). Hatched areas and vectors show significant regressions at 90% confidence. The Pacific Walker Circulation index is defined as the east-west difference between the annual sea-level pressure averaged over the central and eastern equatorial Pacific (160°W–80°W, 5°S–5°N) and over the equatorial Indian Ocean and western equatorial Pacific (80°E–160°E, 5°S–5°N). The annual circulation and environment are calculated by averaging the monthly data weighted with the seasonality of WNP TC frequency throughout the 12 months.

likely to vary on longer timescales or under global warming, although they are not expected to change substantially. The caveat of this assumption may cause uncertainty in the trend and correlation analysis in this study.

Methods

Best track data and data justification

Tropical cyclone (TC) Best Track observations from four national meteorological agencies —the JMA, the China Meteorological Administration (CMA), the Joint Typhoon Warning Center (JTWC), and the Hong Kong Observatory (HKO) — since 1980 are used in the analysis. TCs formed in the whole year (12 months) are considered. Best Track observations include the location, intensity (maximum sustained wind speed and minimum sea level pressure), and storm stage (subject to agencies) at 6-houly intervals. To exclude the uncertainty in weak storms in the Best Track[42], this study only considers TCs that reach severe tropical storm intensity and above during the lifetime, i.e. the maximum sustained wind speed ≥24.5 m/s. TC genesis location is defined by the first track point where TC intensity reaches 17.5 m/s[27,29]. Note that both JMA and HKO data use 10-min mean for measuring maximum sustained wind speed, and CMA and JTWC use 2-and 1-min means, respectively. This inconsistence could cause uncertainty in counting the number of TC and track points. But I find that the impact on this study is minimal (this will be shown later).

Best Track data from different agencies contain large uncertainty in recording the track points outside of tropical regions. Previous studies indicate that the reliability of TC translation speed at the basin-wide or global scales is highly dependent on the track point sampling in the extra tropics[6,7]. In this study, a procedure for data justification has been implemented to select the Best Track data, by following the two key criteria: (i) the best spatial sampling coverage in the subtropics, and (ii) the sample size of track points in the tropics and subtropics has no abrupt changes with time. The data justification procedure is based on the common period of 1980–2021 when all datasets have available data. Please note that when this study is being carried out, the JMA data are available in a longer period of 1980–2023.

The four data sources are consistent in recording the number of TCs in the whole basin (Supplementary Fig. 11), suggesting that variations in counting TCs at severe tropical storm intensity and above are small and have minimal impact. For the track points, within the four data sources, the JMA data contain the highest number of track points (by either per storm or per year) in the whole basin. I then calculate the sampling number falling within various latitude bands. Clearly, in the tropics (0–20°N), the sampling number is homogeneous among different data sources (Supplementary Fig. 12), affirming that the variations in TC intensity identification have minimal impact on the sampling in the deep tropics. In regions beyond the tropics (20–60°N), the JMA data have an average of 177 points higher sampling (62% higher) compared to the other three datasets. Although the discrepancies seem slightly smaller in 1980–1990, the reduction is not substantial. Over 1980–2021, the sampling numbers in the tropics have a weak decreasing trend related to the fewer storms associated with a strengthening of the PWC[29]. There are no abrupt long-term changes in the sampling numbers in the higher latitude bands.

I then confirm that the disparity of the sampling numbers in the higher latitudes among the four data sources is mostly from the TCs that underwent the extratropical transition (ET). In the WNP, towards higher latitudes in the decaying phases of the storm, 49% of TCs underwent the ET[32,33]. For example, in the JMA data, the mean value of minimum sea level pressure in 24 h before the ET starts is on average 7.2 hPa lower than the value in 24 h after. The four data sources consider track recording differently in the extratropical cyclone (EC) stage after the ET completes. JMA continues to record track data in the EC stage, while CMA and other centres have much shorter record or stop recording immediately after ET in many TC cases[33]. Supplementary Fig. 13 shows the number of track points recorded as in the EC stage of the TC lifecycle. In the EC stage, on average, the JMA data have up to 100 track points (per year) more than the CMA and JTWC data. Note that JTWC started the EC recording from 2004 and the HKO data do not explicitly include the EC stage[4,33]. Additionally, the four datasets have different definitions about when the ET process starts and complete[33]. The timing of ET in the JMA data on average is later than that in other datasets. This means that the EC track points in Supplementary Fig. 13 do not entirely explain the difference in the overall track points in Supplementary Fig. 12. In the WNP when moving to the higher latitudes, over 80% of recurving TCs underwent the ET process and become ECs[30]; Best Track data are more certain in recording TC recurvature than in recording the timing of ET. Thus, it is fair to expect that the difference of track points after the recurvature point will broadly indicate the overall EC track difference which is less sensitive to the ET criteria being used in different agencies, and that this identification is more homogeneously recorded in these agencies. This is tested in Supplementary Fig. 14, which shows that after the recurvature point the JMA data have 134 points (per year) more than the other three datasets. I also calculated the track point sampling during the whole lifecycle of TC, conditional on recurving or non-recurving TCs (not shown). I found that the disparity of the track point sampling among the four data sources can be well explained by the sampling for recurving TCs. Thus, the EC stage that is mostly seen in recurving TCs is the main source of uncertainty in the four Best Track datasets[4]. Following refs. 29,43, recurving TCs meet the following selection criteria: (1) storm recurves east at the westernmost point over the full lifetime; (2) the subsequent track point is further north than the

recurving point. Non-recurving TCs are the storms that do not simultaneously meet above two criteria.

To compare with the climatology and trends in TC translation speed at each latitude band produced from the JMA data, I also repeat the same analysis using the JMA, CMA, JTWC, and HKO data, separately. TC translation speed and track point counting at the 10° latitude-moving bands are defined in the following section. Supplementary Fig. 15 shows the climatology and trends of TC translation speed and track density at the 10° latitude-moving bands from 0 to 60°N, over 1980–2021. As expected, because of the low data sampling in the higher latitudes, the CMA, JTWC, and HKO data show divergent climatology of TC translation speed and show insignificant long-term trends above 20°N. In contrast, the climatology and trends in the tropics seen in the JMA data are well re-produced in other three data. Also, the recurving TCs are responsible for such uncertainty in detecting the regional trends of translation speed in the subtropics (Supplementary Figs. 16 and 17). When the overall EC stage is not considered, the trends of translation speed at the latitude bands mostly disappear in the JMA data and become more consistent with other datasets (Supplementary Fig. 18). These affirm that the sampling number in the whole lifecycle of TC is crucial to detect reliable long-term changes in TC translation speed as suggested in previous studies[6,7].

Lastly, the long-term changes in TC track metrics at the basin-wide scale are justified. See the following section for the definition of the basin-wide TC track metrics. Although the poleward migration of TCs is significant in all the Best Track datasets, the migrating rates in the JTWC and HKO data are smaller (Supplementary Table 3). These smaller migrating rates could be related to the low data sampling especially for recurving TCs in the subtropics as well (Supplementary Figs. 15 and 16). In other words, for the annual-mean location, the JTWC and HKO datasets give much greater weight to the low-latitude TC tracks, and consequently they are less able to capture the seesaw-like distribution of the relative track density trends between the low and high latitudes. Thus, due to the smaller migrating rates, the component of the basin-wide translation speed related to the track shift has no significant changes in the JTWC and HKO data (Supplementary Table 3). The component of the basin-wide translation speed related just to regional translation speed has negative trends in all the datasets, but the trends in the CMA, JTWC, and HKO data are not significant due to the poor sampling coverage in the subtropics, as discussed earlier. Hence, the CMA, JTWC, and HKO data show weak or absent trends in basin-wide translation speed due to the low data sampling in the subtropical regions.

Based on the above justification, due to its best sampling coverage in the subtropics in the late stage of the TC lifecycle, the JMA data have been selected as the main dataset for studying the basin-wide relationship between the poleward migration and the translation speed slowdown of TCs. Please note that to employ a longer data record, the JMA data spanning 1980–2023 are used in the Results section.

TC translation speed and latitudinal position

For each TC, translation speed (km/h) is calculated by using the great-circle distance between two consecutive 6-hourly locations. The latitudinal and longitudinal translation speeds are also calculated by only considering the south-north or west-east movements of the 6-hourly track points. The annual-mean basin-wide translation speed is the average of translation speed at 6-hourly interval, in the whole year (12 months) over the western North Pacific (0–60°N, 100–180°E). Correspondingly, the annual-mean basin-wide latitudinal position of TCs is calculated by averaging the latitude of 6-hourly track points, which are used in estimating the basin-wide translation speed above, in the whole year (12 months) over the ocean basin.

The regional translation speed is calculated at each grid point as the translation speed averaged over an area defined by a 10° × 10° box centred at the grid point, for each year; the sample size used in calculating the regional translation speed at each grid point is the number of track points (track density, number per year) integrated over the 10° × 10° box centred at the grid point. Translation speed at the 10° latitude-moving bands, at 1° interval (unless stated otherwise), from 0 to 60°N for each year is calculated as the average translation speed at the 10° latitude band; the sample size used in calculating the translation speed is the number of track points integrated over the 10° latitude band centred at the latitude point.

Decomposing the basin-wide translation speed

Assuming in year y, there are M TCs in total, and the mth TC of the year has T_m track points at 6-hourly interval. For the t_mth track point of the mth TC, the latitude is denoted as $lat(m, t_m)$, and the corresponding translation speed is denoted as $tcs(m, t_m)$ that is calculated by using the t_mth and $(t+1)_m$th track point of the whole track. The sample size of translation speed at 6-hourly interval for the year is $N = \sum_{m=0}^{M}(T_m - 1)$. Therefore, the annual average of TC translation speed over the basin (named the basin-wide TCS) in year y ($TCS(y)$) can be initially written as:

$$TCS(y) = \frac{\sum_{m=0}^{M}\sum_{t_m=0}^{T_m-1} tcs(m, t_m)}{N} \tag{1}$$

Grouping the N track point samples into 60 latitude bands with 1° interval yields the track density $n(lat)$. The latitude of track points averaged over the basin (named the basin-wide latitude) in year y ($Lat(y)$) is then written as:

$$Lat(y) = \frac{\sum_{lat=0}^{60} lat * n(lat)}{N} = \sum_{lat=0}^{60} lat * f(lat) \tag{2}$$

where $f(lat) = n(lat)/N$, representing the proportion of track density in the latitude band lat.

With the same concept, grouping the N translation speed samples into 60 latitude bands with 1° interval yields the track density $n(lat)$ and the average translation speed $tcs(lat)$ for the latitude band lat. Then, Eq.(1) can be rewritten on a latitudinal base as:

$$TCS(y) = \frac{\sum_{lat=0}^{60} tcs(lat) * n(lat)}{N} = \sum_{lat=0}^{60} tcs(lat) * f(lat) \tag{3}$$

The annual values of $tcs(lat)$ and $f(lat)$ can be partitioned to long-term time means ($\overline{tcs(lat)}$ and $\overline{f(lat)}$) and anomalies deviating from the time means ($tcs'(lat)$ and $f'(lat)$) in year y. This is expressed as:

$$\begin{aligned} tcs(lat) &= \overline{tcs(lat)} + tcs'(lat) \\ f(lat) &= \overline{f(lat)} + f'(lat) \end{aligned} \tag{4}$$

Finally, for year y, the annual average of basin-wide translation speed $TCS(y)$ in Eq. (1) is rewritten to:

$$\begin{aligned} TCS(y) &= \sum_{lat=0}^{60} tcs(lat) * f(lat) \\ &= \sum_{lat=0}^{60} (\overline{tcs(lat)} + tcs'(lat)) * (\overline{f(lat)} + f'(lat)) \\ &= \sum_{lat=0}^{60} \overline{tcs(lat)} * \overline{f(lat)} + \sum_{lat=0}^{60} \overline{tcs(lat)} * f'(lat) \\ &\quad + \sum_{lat=0}^{60} tcs'(lat) * \overline{f(lat)} + \sum_{lat=0}^{60} tcs'(lat) * f'(lat) \\ &= \overline{TCS} + \delta_{p'} + \delta_{TCS'} + \delta_{p'TCS'} \end{aligned} \tag{5}$$

The deviation of annual $TCS(y)$ from the long-term climatic average ($\overline{TCS}$) is formed by the three terms, denoted as $\delta_{p'}$, $\delta_{TCS'}$, and $\delta_{p'TCS'}$, which quantify individual contributions of the interannual effect of regional track density ($f'(lat)$) integrated with the climatology of translation speed ($\overline{tcs(lat)}$) over all latitudes, the interannual effect of regional translation speed ($tcs'(lat)$) integrated with the climatology of track density ($\overline{f(lat)}$) over

all latitudes, and the co-variability of interannual anomalies of regional translation speed and regional track density ($tcs'(lat)$ and $f'(lat)$), respectively.

In other words, $\delta_{p'}$ represents the translation speed deviations from the long-term average ($\overline{TCS}$) by retaining interannual variability of TC track density along the latitudes but keeping the climatology of the translation speed. $\delta_{TCS'}$ represents the translation speed deviations by retaining the interannual variability of translation speed along the latitudes but keeping the climatology of TC track density. The term $\delta_{p'TCS'}$ is a non-linear term, which is small.

Large-scale environmental conditions

This study also investigates large-scale environmental conditions related to TCs. Large-scale environmental steering flow is estimated by averaging horizontal winds over 700, 600, 500, and 400 hPa. Middle-tropospheric geopotential height relative to the global mean is the vertical average of geopotential height over 700, 600, 500, and 400 hPa after the global mean has been removed at each pressure level; following the same definition, middle-tropospheric air temperature relative to the global mean is also estimated. Zonal vertical wind shear is estimated by calculating the absolute values of the difference of zonal wind velocity between 200 and 850 hPa. Other variables at single levels, including sea surface temperature, and relative humidity at 500 hPa, are also used to interpret the changes and variations in TC track. These large-scale environmental conditions are derived from the monthly data in the whole year (12 months) in 1980–2023 in the European Centre for Medium-Range Weather Forecasts (ECMWF) fifth-generation reanalysis (ERA5)[44].

It is fair to use the monthly mean of the middle-tropospheric winds to represent the large-scale steering flow in which TCs are embedded at synoptic scales[34–37]. In this study, because TC motion in the whole year (12 months) is studied, the annual average of large-scale steering flow is produced. Because WNP TC frequency has a clear seasonal cycle, when computing the annual average of large-scale steering flow, here, the monthly steering flow data are averaged throughout the 12 months and weighted with the monthly proportion (seasonality) of observed TC frequency, referred to as the seasonality-weighted average. A conventional average (e.g. weighted equally at each month) for annual large-scale steering flow is problematic here. This is because the annual TC metrics have more weight on summer TCs than winter TCs, thus environmental condition values associated with TC metrics should be weighted in the same way. In contrast, for a reverse seasonality-weighted average of large-scale steering flow, monthly values have least weight in the months when TC occurs climatologically often and have most weight in the months when TCs are climatologically rare. The reverse seasonality-weighted average minimizes the TC impact on large-scale steering flow, reflecting the conditions that are independent of TC appearance. Supplementary Fig. 19 shows the weighting scores used in calculating the seasonality-weighted and reverse seasonality-weighted annual averages. These seasonality-weighted averages are applied to other environmental conditions in this study.

Climate and Walker Circulation indices

The El Niño Southern Oscillation (ENSO) index is defined by the monthly standardized sea surface temperature anomalies averaged in the Niño 3.4 region (5°S–5°N, 170°W–120°W). The Pacific Decadal Oscillation (PDO) index is defined as the leading principal component of North Pacific monthly sea surface temperature variability (poleward of 20°N). Yearly ENSO and PDO indices are integrals of the monthly indices weighted with the monthly proportion of observed WNP TC frequency throughout the 12 months.

The PWC index is defined as the east-west difference between the sea-level pressure averaged over the central and eastern equatorial Pacific (160°W–80°W, 5°S–5°N) and over the equatorial Indian Ocean and western equatorial Pacific (80°E–160°E, 5°S–5°N)[45]. The PWC index is derived from the annual sea-level pressure in ERA5. The annual sea-level pressure is computed by integrating the monthly data weighted with the monthly proportion of observed WNP TC frequency throughout the 12 months.

Statistical analyses

For the trend analysis, I estimate the trend (denoted as b) using a linear least-squares regression and also estimate the error bars (denoted as err) of the trend by a two-tailed 95% confidence interval under the assumption that the residuals of the regression follow a normal distribution. $b \pm$ err represents the 95% confidence estimate of the trend value. The trend is tested for statistical significance for a null hypothesis that the trend is zero (i.e. a significant trend means that the interval of trend ($b \pm$ err) does not include zero).

The Pearson correlation coefficient (denoted as r) is used to measure the correlation between the time series of two variables after removing the linear trends. A two-tailed t-test with p-value of 0.05 is used to test significance, with a null hypothesis of a zero correlation. In other words, in this paper, the statistically significant values (b or r) are at the 95% confidence level, unless stated otherwise.

Before implementing the above statistical analyses (i.e. trend and correlation calculations), the effects of the ENSO and PDO are removed from the time series of TC metrics and environmental variables, as suggested in refs. 25,26,29. To do so, a multiple linear regression on the yearly ENSO and PDO indices with a linear least-squares method is first estimated for the time series of data. The values determined by ENSO and PDO indices are then removed from the time series of TC or environmental data, to obtain the residuals. The residuals feed into the above trend and correlation analyses. This means that the teleconnections from ENSO and PDO to WNP TC metrics (i.e. translation speed, and position) and large-scale environment are eliminated in this paper, assuming that these relationships are stationary with time.

Data availability

Best Track data are obtained from four national meteorological agencies, which are the Japan Meteorological Agency (JMA; www.jma.go.jp/jma/jma-eng/jma-center/rsmc-hp-pub-eg/trackarchives.html), the China Meteorological Administration (CMA; http://tcdata.typhoon.org.cn/en/zjljsjj_sm.html), the Joint Typhoon Warning Center (JTWC; https://www.metoc.navy.mil/jtwc/jtwc.html?best-tracks), and the Hong Kong Observatory (HKO; https://data.gov.hk/en-data/dataset/hk-hko-rss-tc-track-info). Monthly ENSO and PDO indices are retrieved from the NOAA's National Centres for Environmental Information (www.ncdc.noaa.gov/teleconnections/). The ERA5 data used in this study are generated by ECMWF and distributed by Copernicus Climate Change Service (C3S) Climate Data Store (CDS) (https://doi.org/10.24381/cds.bd0915c6). Computing and data storage facilities were provided by JASMIN (https://jasmin.ac.uk).

Code availability

The codes used to analyse the data and to generate the plots in this paper are available from the corresponding author on request.

Received: 27 November 2023; Accepted: 14 August 2024;
Published online: 24 August 2024

References

1. Kossin, J. P. A global slowdown of tropical-cyclone translation speed. *Nature* **558**, 104–107 (2018).
2. Knapp, K. R. & Kruk, M. C. Quantifying interagency differences in tropical cyclone best-track wind speed estimates. *Mon. Weather Rev.* **138**, 1459–1473 (2010).
3. Barcikowska, M., Feser, F. & Von Storch, H. Usability of best track data in climate statistics in the western North Pacific. *Mon. Weather Rev.* **140**, 2818–2830 (2012).

4. Ying, M. et al. An overview of the China Meteorological Administration tropical cyclone database. *J. Atmos. Ocean. Technol.* **31**, 287–301 (2014).
5. Velden, C. et al. The Dvorak tropical cyclone intensity estimation technique: a satellite-based method that has endured for over 30 years. *Bull. Am. Meteorol. Soc.* **87**, 1195–1210 (2006).
6. Lanzante, J. R. Uncertainties in tropical-cyclone translation speed. *Nature* **570**, E6–E15 (2019).
7. Moon, I. J., Kim, S. H. & Chan, J. C. Climate change and tropical cyclone trend. *Nature* **570**, E3–E5 (2019).
8. Chang, Y. T., Lin, I. I., Huang, H. C., Liao, Y. C. & Lien, C. C. The association of typhoon intensity increase with translation speed increase in the South China Sea. *Sustainability* **12**, 939 (2020).
9. Wang, C. et al. Interannual variability of the basinwide translation speed of tropical cyclones in the western North Pacific. *J. Clim.* **33**, 8641–8650 (2020).
10. Zhang, D. et al. Changes in tropical-cyclone translation speed over the western North Pacific. *Atmosphere* **11**, 93 (2020).
11. Yamaguchi, M. & Maeda, S. Slowdown of typhoon translation speeds in mid-latitudes in September influenced by the Pacific decadal oscillation and global warming. *J. Meteorol. Soc. Jpn. Ser. II* **98**, 1321–1334 (2020).
12. Seneviratne, S. I. et al. Weather and climate extreme events in a changing climate. in *Climate Change 2021: The Physical Science Basis. Contribution of Working Group I to the Sixth Assessment Report of the Intergovernmental Panel on Climate Change* [eds Masson-Delmotte, V., P. Zhai, A. Pirani, S. L. Connors, C. Péan, S. Berger, N. Caud, Y. Chen, L. Goldfarb, M. I. Gomis, M. Huang, K. Leitzell, E. Lonnoy, J. B. R. Matthews, T. K. Maycock, T. Waterfield, O. Yelekçi, R. Yu, and B. Zhou] (Cambridge University Press, 2021) https://doi.org/10.1017/9781009157896.013.
13. Chu, P. S., Kim, J. H., & Ruan Chen, Y. (2012). Have steering flows in the western North Pacific and the South China Sea changed over the last 50 years? *Geophys. Res. Lett.* **39**, 10704 (2012).
14. Coumou, D., Lehmann, J. & Beckmann, J. The weakening summer circulation in the Northern Hemisphere mid-latitudes. *Science* **348**, 324–327 (2015).
15. Screen, J. A. et al. Consistency and discrepancy in the atmospheric response to Arctic sea-ice loss across climate models. *Nat. Geosci.* **11**, 155–163 (2018).
16. Vihma, T. Effects of Arctic sea ice decline on weather and climate: a review. *Surv. Geophys.* **35**, 1175–1214 (2014).
17. Ma, S. & Zhou, T. Robust strengthening and westward shift of the tropical Pacific Walker circulation during 1979–2012: a comparison of 7 sets of reanalysis data and 26 CMIP5 models. *J. Clim.* **29**, 3097–3118 (2016).
18. De Boisséson, E., Balmaseda, M. A., Abdalla, S., Källén, E. & Janssen, P. A. E. M. How robust is the recent strengthening of the tropical Pacific trade winds? *Geophys. Res. Lett.* **41**, 4398–4405 (2014).
19. Li, Y. et al. Long-term trend of the tropical Pacific trade winds under global warming and its causes. *J. Geophys. Res. Oceans* **124**, 2626–2640 (2019).
20. Sohn, B. J., Yeh, S. W., Schmetz, J. & Song, H. J. Observational evidences of Walker circulation change over the last 30 years contrasting with GCM results. *Clim. Dyn.* **40**, 1721–1732 (2013).
21. L'Heureux, M. L., Lee, S. & Lyon, B. Recent multidecadal strengthening of the Walker circulation across the tropical Pacific. *Nat. Clim. Change* **3**, 571–576 (2013).
22. Chung, E. S. et al. Reconciling opposing Walker circulation trends in observations and model projections. *Nat. Clim. Change* **9**, 405–412 (2019).
23. Seager, R. et al. Strengthening tropical Pacific zonal sea surface temperature gradient consistent with rising greenhouse gases. *Nat. Clim. Change* **9**, 517–522 (2019).
24. Woollings, T., Drouard, M., O'Reilly, C. H., Sexton, D. M. & McSweeney, C. Trends in the atmospheric jet streams are emerging in observations and could be linked to tropical warming. *Commun. Earth Environ.* **4**, 125 (2023).
25. Kossin, J. P., Emanuel, K. A. & Vecchi, G. A. The poleward migration of the location of tropical cyclone maximum intensity. *Nature* **509**, 349–352 (2014).
26. Kossin, J. P., Emanuel, K. A. & Camargo, S. J. Past and projected changes in western North Pacific tropical cyclone exposure. *J. Clim.* **29**, 5725–5739 (2016).
27. Daloz, A. S. & Camargo, S. J. Is the poleward migration of tropical cyclone maximum intensity associated with a poleward migration of tropical cyclone genesis? *Clim. Dyn.* **50**, 705–715 (2018).
28. Knutson, T. et al. Tropical cyclones and climate change assessment: Part I: detection and attribution. *Bull. Am. Meteorol. Soc.* **100**, 1987–2007 (2019).
29. Feng, X., Klingaman, N. P. & Hodges, K. I. Poleward migration of western North Pacific tropical cyclones related to changes in cyclone seasonality. *Nat. Commun.* **12**, 6210 (2021).
30. Archambault, H. M., Bosart, L. F., Keyser, D. & Cordeira, J. M. A climatological analysis of the extratropical flow response to recurving western North Pacific tropical cyclones. *Mon. Weather Rev.* **141**, 2325–2346 (2013).
31. Keller, J. H. et al. The extratropical transition of tropical cyclones. Part II: Interaction with the midlatitude flow, downstream impacts, and implications for predictability. *Mon. Weather Rev.* **147**, 1077–1106 (2019).
32. Kitabatake, N. Climatology of extratropical transition of tropical cyclones in the western North Pacific defined by using cyclone phase space. *J. Meteorol. Soc. Jpn. Ser. II* **89**, 309–325 (2011).
33. Sun, H. M., Lei, X. T., Tang, J., Yao, C. & Luo, X. L. Comparisons of the characteristics of tropical cyclones experiencing extratropical transition in the western North Pacific based on different datasets. *J. Trop. Meteorol.* **23**, 281–291 (2017).
34. Holland, G. J. *Tropical cyclone motion: Environmental interaction plus a beta effect* (Department of Atmospheric Science, Colorado State University, 1982).
35. Wu, L. & Wang, B. Assessment of global warming impacts on tropical cyclone track. *J. Clim.* **17**, 1686–1698 (2004).
36. Zhao, H., Wu, L., & Zhou, W. Observational relationship of climatologic beta drift with large-scale environmental flows. *Geophys. Res. Lett.* **36**, L18809 (2009).
37. Lu, J., Wu, L., Zhou, S. & Zhao, H. Interannual variations of the β drift of tropical cyclones over the western North Pacific. *J. Clim.* **36**, 745–752 (2023).
38. Fiorino, M. & Elsberry, R. L. Some aspects of vortex structure related to tropical cyclone motion. *J. Atmos. Sci.* **46**, 975–990 (1989).
39. Yeh, S. W. et al. Decadal change in relationship between western North Pacific tropical cyclone frequency and the tropical Pacific SST. *Meteorol. Atmos. Phys.* **106**, 179–189 (2010).
40. Kim, M. H., & Moon, I. J. Evaluation of the reliability of tropical cyclone data using ENSO. *Asia-Pacific J. Atmos. Sci.* **58**, 1–13 (2022).
41. Zhao, H. & Wang, C. Interdecadal modulation on the relationship between ENSO and typhoon activity during the late season in the western North Pacific. *Clim. Dyn.* **47**, 315–328 (2016).
42. Torn, R. D. & Snyder, C. Uncertainty of tropical cyclone best-track information. *Weather Forecast.* **27**, 715–729 (2012).
43. Zhang, W., Leung, Y. & Chan, J. C. The analysis of tropical cyclone tracks in the western North Pacific through data mining. Part I: tropical cyclone recurvature. *J. Appl. Meteorol. Climatol.* **52**, 1394–1416 (2013).
44. Hersbach, H. et al. The ERA5 global reanalysis. *Q. J. R. Meteorol. Soc.* **146**, 1999–2049 (2020).
45. Vecchi, G. A. et al. Weakening of tropical Pacific atmospheric circulation due to anthropogenic forcing. *Nature* **441**, 73–76 (2006).

Acknowledgements
X.F. was supported by the Singapore Green Finance Centre, the UK Met Office Weather and Climate Science for Service Partnership for Southeast Asia (H5480800, H5525000) as part of the Newton Fund, and the National Centre for Atmospheric Science through the NERC National Capability International Programmes Award (NE/X006263/1).

Author contributions
X.F. designed and performed the research; X.F. wrote the manuscript.

Competing interests
The author declares no competing interests.

Additional information
Supplementary information The online version contains supplementary material available at https://doi.org/10.1038/s41612-024-00748-5.

Correspondence and requests for materials should be addressed to Xiangbo Feng.